Journal Pre-proof

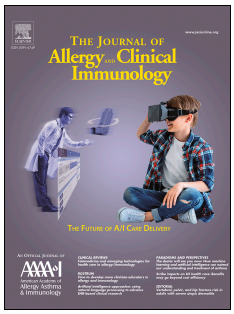

Probiotics-derived metabolite ameliorates skin allergy by promoting differentiation of FOXP3^{+} regulatory T cells

Hye-Ji Kang, PhD, Gi-Cheon Kim, PhD, Choong-Gu Lee, PhD, Sunhee Park, Bs, Garima Sharma, PhD, Ravi Verma, PhD, Sin-Hyoeg Im, PhD, Ho-Keun Kwon, PhD

PII: S0091-6749(20)31727-9

DOI: https://doi.org/10.1016/j.jaci.2020.11.040

Reference: YMAI 14877

To appear in: *Journal of Allergy and Clinical Immunology*

Received Date: 19 November 2019

Revised Date: 20 October 2020

Accepted Date: 25 November 2020

Please cite this article as: Kang H-J, Kim G-C, Lee C-G, Park S, Sharma G, Verma R, Im S-H, Kwon H-K, Probiotics-derived metabolite ameliorates skin allergy by promoting differentiation of FOXP3^{+} regulatory T cells, *Journal of Allergy and Clinical Immunology* (2021), doi: https://doi.org/10.1016/j.jaci.2020.11.040.

Probiotics-derived metabolite ameliorates skin allergy by promoting differentiation of FOXP3^{+} regulatory T cells

Authors

Hye-Ji Kang, PhD[1,2*], Gi-Cheon Kim, PhD[3,4*], Choong-Gu Lee, PhD[5*], Sunhee Park, Bs[6], Garima Sharma, PhD[6], Ravi Verma, PhD[6], Sin-Hyoeg Im, PhD[6,7#], Ho-Keun Kwon, PhD[3,4,8#]

[1] Advanced Green Energy and Environment Institute (AGEE), Handong Global University, Pohang 37554, Republic of Korea

[2] HEM, Handong-ro 558, Pohang-si, Gyungbuk, 37554, Republic of Korea

[3] Department of Microbiology and Immunology, Yonsei University College of Medicine, 50-1 Yonsei-ro, Seodaemun-gu Seoul, Seoul 03722, Korea

[4] Institute for Immunology and Immunological Diseases, Yonsei University College of Medicine, Seoul 03722, Korea

[5] Natural Product Informatics Research Center, Korea Institute of Science and Technology (KIST), Gangneung Institute of Natural Products, Gangneung, Gangwon-do, 25451, Republic of Korea

[6] Immunobiome, Pohang University of Science and Technology Biotech Center, Pohang 37673, Republic of Korea

[7] Division of Integrative Biosciences and Biotechnology (IBB), Department of Life Sciences, Pohang University of Science and Technology (POSTECH), Pohang 37673, Republic of Korea

[8] Brain Korea 21 PLUS Project for Medical Sciences, Yonsei University College of Medicine, Seoul 03722, Korea

* equally contributing first authors, # equally contributing corresponding authors

#Correspondence: HK@yuhs.ac

Department of Microbiology and Immunology, Yonsei University College of Medicine, 50-1 Yonsei-ro, Seodaemun-gu Seoul, Seoul 03722, Korea

Phone: 82-2-2228-1818/Fax: 82-2-392-7088

Sources of funding: This work was funded by National Research Foundation of Korea (NRF) grants (2018M3A9F3021964, 2019R1A6A1A03032869, 2019R1F1A1060415, 2019M3C9A6091949), Korea Institute of Science and Technology intramural grants (2Z06220 and 2Z06130), a new faculty research seed money grant of Yonsei University College of Medicine for 2019 (2019-32-0022), and a faculty research grant of Yonsei University College of Medicine (6-2019-0113).

Conflict of Interest: GS and RV are employed by company ImmunoBiome. S-HI is the CEO of ImmunoBiome. These authors declare no conflicts of interest for this paper as the research was conducted without any commercial or financial relationships. The remaining authors declare no conflict of interest.

Short (Capsule) summary: This study showed the novel action mechanism of probiotics that promote the production of propionate, which is critical for $FOXP3^+$ regulatory T cells induction and anti-inflammatory effects suggesting potential as alternative therapeutics for skin allergies.

Key words: Probiotics, Short chain fatty acids, Regulatory T cell, Skin allergies

To the Editor

Probiotics has shown their potent immuno-modulatory effects and is considered as promising alternative for the prevention and treatment of inflammatory disorders[1]. However, lack of precise action mechanisms of probiotics restrained their application especially for the treatment of non-gastrointestinal diseases such as skin allergies including atopic dermatitis and allergic contact dermatitis[2]. Previously, we have shown that the combination of rationally selected five probiotic bacteria strains (known as IRT5) has persuasive therapeutic effects on autoimmunity[3]. However, it is still unclear how oral supplementation of IRT5 modulates immune system and eventually has therapeutic efficacy in skin allergies such as contact dermatitis and atopic dermatitis.

Here, we have investigated the action mechanisms of IRT5 for the induction of $FOXP3^+$ Treg cells (Tregs) and the resolution of skin inflammations in hapten-induced contact hypersensitivity (CHS) as well as house dust mite induced atopic dermatitis (AD) as type 1 and type 2-inflammatory skin allergic models respectively[4]. Consistent with known immuno-pathology of CHS, the topical single (Fig. 1A) or repeated challenges (Fig. 1B) of hapten (2,4-Dinitrochlorobenzene: DNCB) provoked severe skin swelling accompanied with intensive infiltration of mononuclear cells (Fig. 1B). Prophylactic treatment of IRT5 significantly mitigated severity of CHS via sensitization (Fig. 1A) along with elicitation phages (Fig. 1B) by suppressing the infiltration of inflammatory innate immune cells (Fig. E1A) and pathogenic cytokines (IL-1β, IL-6, IL-17A, IL-23, and TNF-α) in inflamed lesion (Fig. 1C, D) as well as in serum (Fig. 1E). Consistently, oral administration of IRT5 significantly suppressed IFN-ɣ and IL-17A production in $CD4^+$ (Fig. E1B) and $CD8^+$ (Fig. E1C) T cells indicating subdued pathogenic T_H1/T_H17 type inflammation by IRT5 administration.

As the previous observation[3], oral administration of IRT5 in CHS-induced mice significantly increased Tregs in inflamed tissue (Fig. 1F), draining lymph nodes (dNLs), and small intestine (SI) (Fig. E2A, B). Interestingly, IRT5 administration seems to specifically enhance generation of peripherally induced Treg cells (HELIOS$^-$ NRP1$^-$ FOXP3$^+$ Tregs) in CHS-induced mice in SPF (Fig. 1G). Single administration of IRT5 in GF mice significantly enhanced NRP1$^-$HELIOS$^-$ pTregs in SI and colon (Fig. 1H and Fig. E3). To further prove that IRT5 administration induces pTregs, we have performed two different experiments. Indeed, we found that adoptively transferred naïve CD4$^+$ T cells could be converted into Treg cells by IRT5 administration in GF mice (Fig. E4A, B). To further prove whether IRT5 could convert naïve T cells into RORγt$^+$FOXP3$^+$ Tregs, we performed co-transfer experiment in which allelically marked naïve CD4$^+$ T cells from WT or *Rorc*^{flox}/*Foxp*3^{cre} mice, lacking microbes-induced pTregs[5], into *Rag1*$^{-/-}$ host. Indeed, we found that exclusive conversion of naïve T cells into pTregs from WT but not from *Rorc*^{flox}/*Foxp3*^{cre} mice by IRT5 treatment (Fig. E4C, D). These data collectively indicate that IRT5 administration enhances the generation of peripherally induced Treg cells. Together with quantitative expansion of Tregs, IRT5 qualitatively modulated Tregs by enhancing Tregs' effector molecules such as CTLA-4 (Fig. 1I) and IL-10 (Fig. 1J) than control group. Intriguingly, we found that transient depletion of Tregs during the course of CHS induction completely abrogated the therapeutic potency of IRT5 in reducing ear thickness and serum TNF-α level, indicating the bona fide protective role of Tregs in allergic contact dermatitis and atopic dermatitis (Fig. 1K-N, Fig E5). Furthermore, likewise CHS, treatment of IRT5 has shown potent therapeutic effects in atopic dermatitis (AD) by suppressing pathogenic T_H2 inflammation, infiltration of inflammatory monocytes and neutrophils while promoting expansion of Tregs which

may not be as the result of long-term colonization of IRT5 (Fig. E6G). Collectively, these indicate potent therapeutic effects of IRT5 as the intrinsic pTregs augmenter in skin allergies.

How does IRT5 promote the expansion of pTregs? Since we could not observe a significant alteration of overall microbiome composition by IRT5 (Fig. E7), we hypothesized IRT5 might directly promote the expansion of pTregs. Recent studies have shown pivotal role of gut commensal to produce short chain fatty acids (SCFAs), mainly from microbial fermentative activity, that have potent immuno-modulatory activities especially on Tregs[6-8]. However, there is still no direct evidence showing that enhanced SCFAs by administration of specific bacteria could upregulate Tregs cells in allergic disorders. Intriguingly, we observed that oral administration of IRT5 specifically promoted the relative production of propionate but not acetate and butyrate in gut of CHS mice compared with vehicle-treated counterpart (Fig. 2A). Furthermore, gnotobiotic colonization of IRT5 in GF mice was sufficient to promote propionate (Fig. 2B) but not butyrate production (Fig. E8A, B), indicating intrinsic capacity of IRT5 to produce propionate. Then, to identify the major contributor for propionate production by IRT5, we mono-colonized each strain of IRT5 and monitored alternation of major SCFAs in gut of GF mice. Consistent with SPF setting, none of bacteria induced butyrate production, well-known for the expansion/generation of Tregs[6, 7] (Fig. E8A). Interestingly, *L. reuteri* (LR) mono-colonization specifically enhanced propionate level in gut indicating the key role of LR in propionate production by IRT5 (Fig. E8B).

To validate whether propionate, induced by IRT5, promotes expansion/generation of Tregs, we pretreated mock (PBS) or propionate on $CD11c^+$ DCs, co-cultured them with naïve $CD4^+$ T cells. Intriguingly, propionate treated DCs

preferentially differentiated naïve $CD4^+$ T cells into $FOXP3^+$ Tregs compared with PBS treated DCs (Fig. 2C). Since both DCs and T cells expressing GPR43, the receptor for propionate (Fig. E9), we directly treated propionate in naïve $CD4^+$ T cells and confirmed significantly enhanced Tregs differentiation upon TGF-β1 stimulation (Fig. 2D). Consistently, treatment of propionate significantly enhanced histone acetylation on Foxp3 promoter as well as CNS1 locus, which are important for the peripheral induction of FOXP3 (Fig. 2E and Fig. E10)[9]. However, co-treatment of A-485, the HAT inhibitor, with propionate significantly abolished Tregs induction as well as histone acetylation on Foxp3 promoter (Fig. 2D, E) indicating the causality of histone acetylation up on propionate treatment for Tregs expansion. Altogether, these suggest that propionate directly modulates dendritic cells as well as $CD4^+$ T cells to intensify pTregs differentiation. Interestingly, propionate specifically curtailed inflammatory responses by T cells (Fig. 2F) but not by other innate cells such as neutrophil and monocyte (Fig. E11) indicating cell type specific effects of individual SCFA. Furthermore, likewise CHS, propionate treatment potently suppressed pathogenic cytokines (IL-4, IL-5, and TNF-α) in $CD4^+$ T cells from AD induced mice (Fig. E12). Altogether, these indicate potential mechanisms of propionate to suppress skin inflammations by directly acting on T cells. To further test whether propionate could recapitulate the protective effect of IRT5 *in vivo*, we orally gavaged mice with vehicle or LR, the major propionate inducer in IRT5, under CHS and AD progression. However, LR alone failed to mimic the therapeutic potency of IRT5 (Fig. E13), suggesting that an immunological synergism among bacterial strains in IRT5 may mediate therapeutic potency of IRT5. Then, we decided to use orphan G-protein-coupled receptors 43, one of major receptor for propionate, deficient mice (*Gpr*43 KO)[8]. Discordant with WT shown in Fig. 1, oral supplementation of IRT5 in

*Gpr*43 KO failed to suppress pathogenesis of hapten-induced CHS (Fig. 2G) accompanied with impaired expansion of pTregs (Fig. 2H), resulting in uncontrolled IFN-ɣ production in $CD4^+$ (Fig. E14A) and $CD8^+$ T cells (Fig. E14B). Thus, these results indicate that propionate is the key immuno-modulatory metabolite induced by IRT5 for the Tregs expansion and mitigating skin inflammation in CHS.

Taken together, our study has given the answer for the fundamental question how IRT5 (multi-strain probiotics) can be the alternative therapeutics for the prevention and treatment of skin allergies. Together with our recent studies[3], we describe a series of novel anti-inflammatory cascades triggered by oral administration of IRT5; 1) IRT5 preferentially induces the production of propionate in the gut. 2) Propionate directly acts on naïve $CD4^+$ T cells to promote pTregs differentiation or indirectly impacts on $CD11c^+$ DC to endow regulatory function to promote the conversion of naïve $CD4^+$ T cells into pTregs. 3) In addition to pTregs expansion, propionate directly influences on effector T cells to suppress allergen-induced inflammations. Importantly, all of these beneficial effects by IRT5 were disappeared by depletion of Tregs or in *Gpr*43 KO mice. In short, this study enlightens novel cellular and molecular pathways involved in the regulation of skin allergies by Tregs inducing multi-probiotic strains and has shown their potentials as alternative therapeutics for the treatment of a broad spectrum of skin allergies.

Hye-Ji Kang, PhD[1,2*],

Gi-Cheon Kim, PhD[3,4*],

Choong-Gu Lee, PhD[5*],

Sunhee Park, Bs[6],

Garima Sharma, PhD[6],

Ravi Verma, PhD[6],

Sin-Hyoeg Im, PhD[6,7#],

Ho-Keun Kwon, PhD[3,4,8#]

[1] Advanced Green Energy and Environment Institute (AGEE), Handong Global University, Pohang 37554, Republic of Korea

[2] HEM, Handong-ro 558, Pohang-si, Gyungbuk, 37554, Republic of Korea

[3] Department of Microbiology and Immunology, Yonsei University College of Medicine, 50-1 Yonsei-ro, Seodaemun-gu Seoul, Seoul 03722, Korea

[4] Institute for Immunology and Immunological Diseases, Yonsei University College of Medicine, Seoul 03722, Korea

[5] Natural Product Informatics Research Center, Korea Institute of Science and Technology (KIST), Gangneung Institute of Natural Products, Gangneung, Gangwon-do, 25451, Republic of Korea

[6] Immunobiome, Pohang University of Science and Technology Biotech Center, Pohang 37673, Republic of Korea

[7] Division of Integrative Biosciences and Biotechnology (IBB), Department of Life Sciences, Pohang University of Science and Technology (POSTECH), Pohang 37673, Republic of Korea

[8] Brain Korea 21 PLUS Project for Medical Sciences, Yonsei University College of Medicine, Seoul 03722, Korea

References

1. Suez J, Zmora N, Segal E, Elinav E. The pros, cons, and many unknowns of probiotics. Nat Med 2019; 25:716-29.
2. Reid G, Jass J, Sebulsky MT, McCormick JK. Potential uses of probiotics in clinical practice. Clin Microbiol Rev 2003; 16:658-72.
3. Kwon HK, Lee CG, So JS, Chae CS, Hwang JS, Sahoo A, et al. Generation of regulatory dendritic cells and CD4+Foxp3+ T cells by probiotics administration suppresses immune disorders. Proc Natl Acad Sci U S A 2010; 107:2159-64.
4. Dhingra N, Gulati N, Guttman-Yassky E. Mechanisms of contact sensitization offer insights into the role of barrier defects vs. intrinsic immune abnormalities as drivers of atopic dermatitis. J Invest Dermatol 2013; 133:2311-4.
5. Sefik E, Geva-Zatorsky N, Oh S, Konnikova L, Zemmour D, McGuire AM, et al. Individual intestinal symbionts induce a distinct population of RORγ+ regulatory T cells. Science 2015; 349:993-7.
6. Arpaia N, Campbell C, Fan X, Dikiy S, van der Veeken J, deRoos P, et al. Metabolites produced by commensal bacteria promote peripheral regulatory T-cell generation. Nature 2013; 504:451-5.
7. Furusawa Y, Obata Y, Fukuda S, Endo TA, Nakato G, Takahashi D, et al. Commensal microbe-derived butyrate induces the differentiation of colonic regulatory T cells. Nature 2013; 504:446-50.
8. Koh A, De Vadder F, Kovatcheva-Datchary P, Backhed F. From Dietary Fiber to Host Physiology: Short-Chain Fatty Acids as Key Bacterial Metabolites. Cell 2016; 165:1332-45.
9. Josefowicz SZ, Lu LF, Rudensky AY. Regulatory T cells: mechanisms of differentiation and function. Annu Rev Immunol 2012; 30:531-64.

Figure legend

Figure 1. Probiotics ameliorate hapten induced contact hypersensitivity. In vehicle or IRT5 treated CHS induced mice, ear thickness upon (A) single or (B) repeated treatment of DNCB and histological changes (H&E staining) were measured. Total cells from inflamed tissue were used to analyze (C) mRNA and (D) protein expression of cytokines. (E) Key pathogenic cytokines of CHS pathogenesis in serum from vehicle or IRT5 treated CHS mice. (F) Frequency of Tregs at inflamed tissue and (G) HELIOS/NRP1 expression in colonic Tregs from vehicle or IRT5 treated CHS mice. (H) Frequency of Tregs in small intestine and colon in vehicle or IRT5 treated germ-free mice. (I) CTLA-4 expression and (J) IL-10 production in dLNs Tregs from of vehicle or IRT5 treated CHS mice. (K) Experimental scheme for Tregs depletion experiment. Upon vehicle or IRT5 treatment with or without Tregs depletion in CHS induced mice, (L) Tregs proportion, (M) ear thickness, and (N) TNF-α in serum were analyzed. Each symbol represents individual animal and performed at least 3 independent experiments. Graphs show mean +/- s.e.m. *$p < 0.05$, ***$p < 0.01$, ***$p < 0.005$ calculated by student t-test.

Figure 2. Probiotics derived propionate suppresses hapten induced skin inflammation. (A) Relative levels of SCFA in fecal contents after treatment of vehicle or IRT5 in CHS mice. (B) Propionate level in GF mice after treatment of vehicle or IRT5. (C) Tregs differentiation of naïve T cells by vehicle (left) or propionate (right) pretreated dendritic cells. (D) TGF-β induced Tregs differentiation

and (E) H3K27 acetylation at *Foxp*3 promoter and CNS1 using ChIP-qPCR upon propionate treatment in the absence or presence A-485. (F) IFN-ɣ production in $CD8^+$ cells by treatment of various SCFAs. (G) Ear thickness and (H) frequency of Tregs at inflamed tissue in CHS induced *Gpr*43 KO mice treated with vehicle or probiotics. Each symbol represents individual animal and performed at least 3 independent experiments. Error bars denote means ± s.e.m. Graphs show mean +/- s.e.m. *p < 0.05, ***p < 0.01, ***p < 0.005 calculated by student t-test.

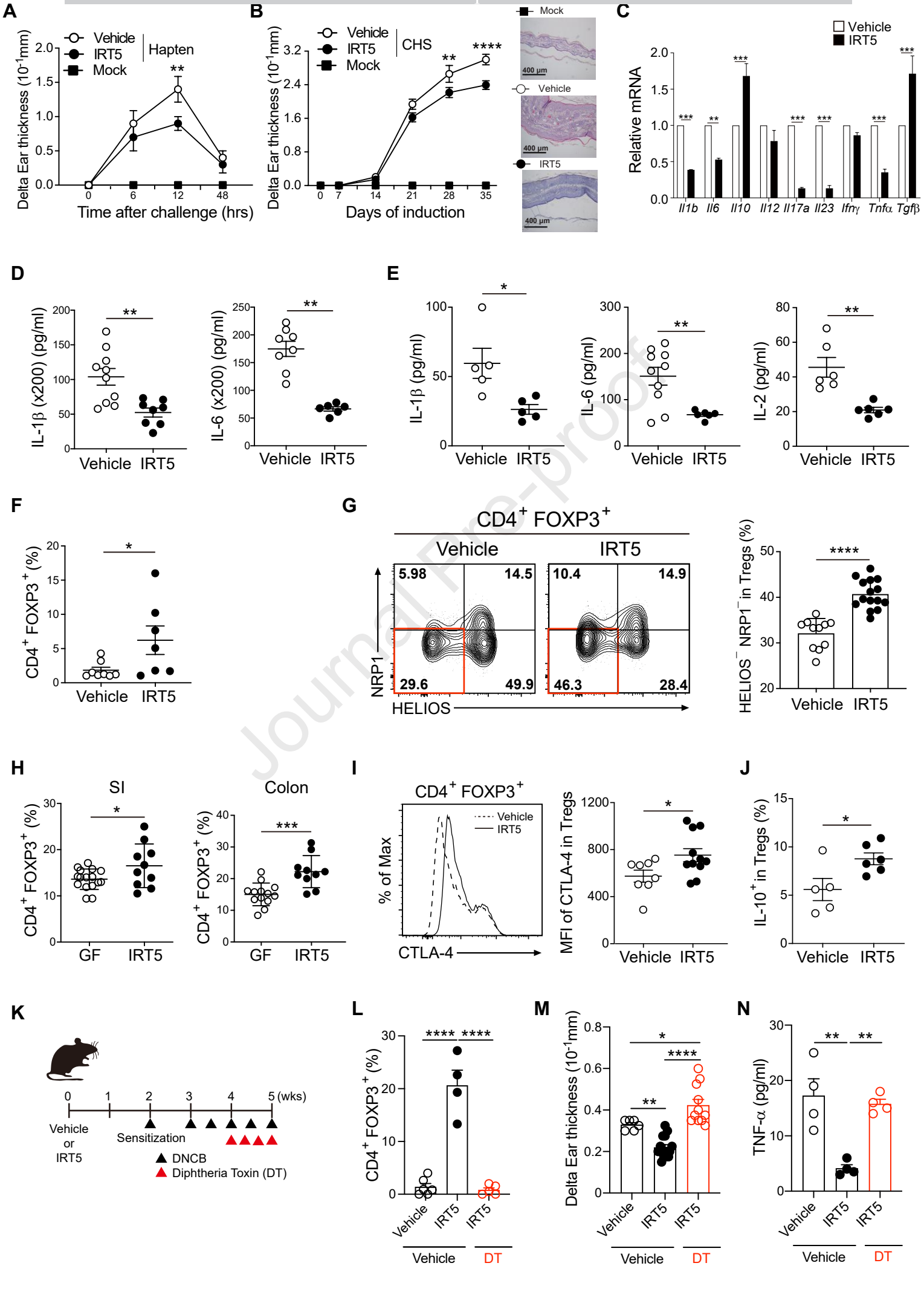

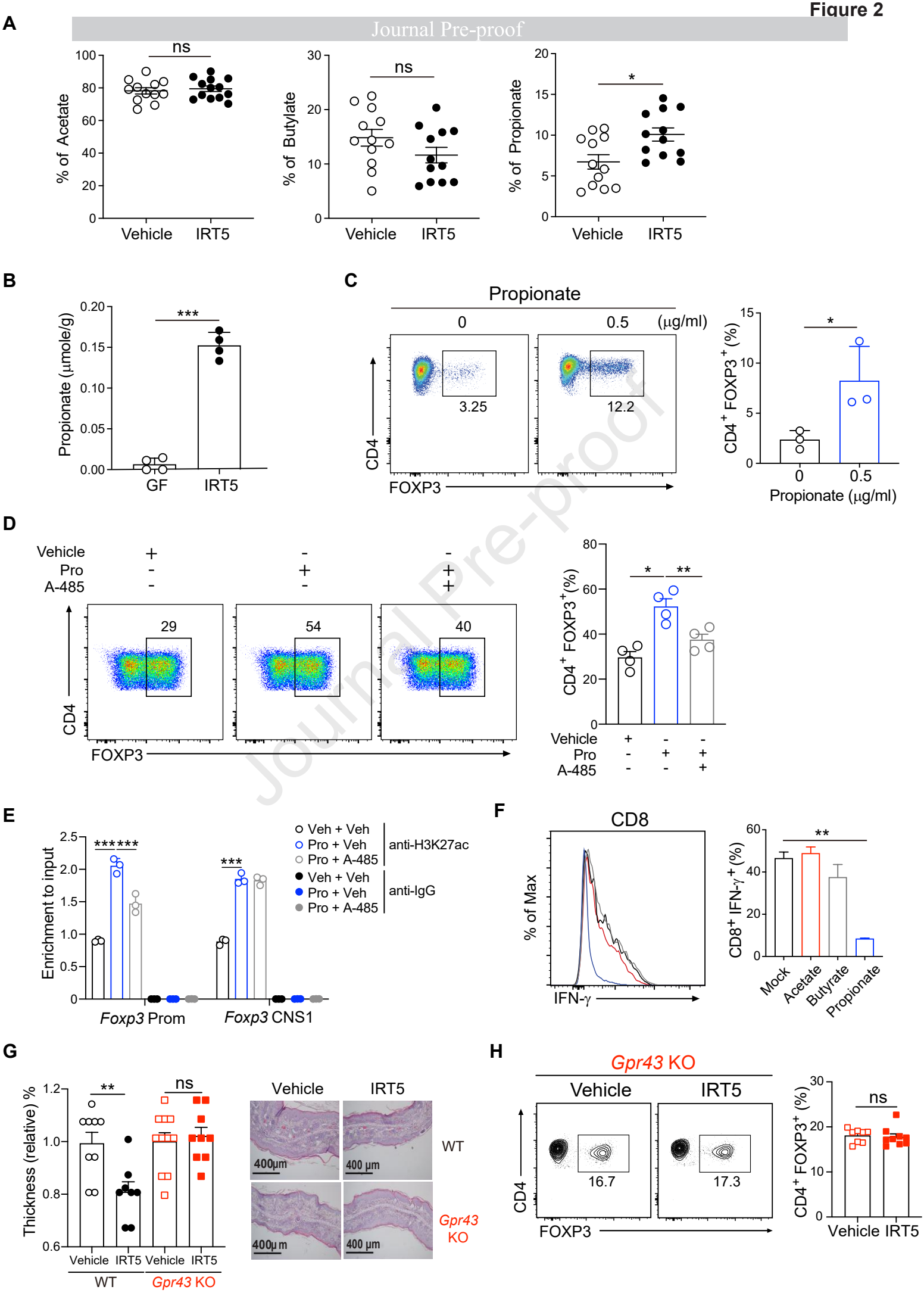

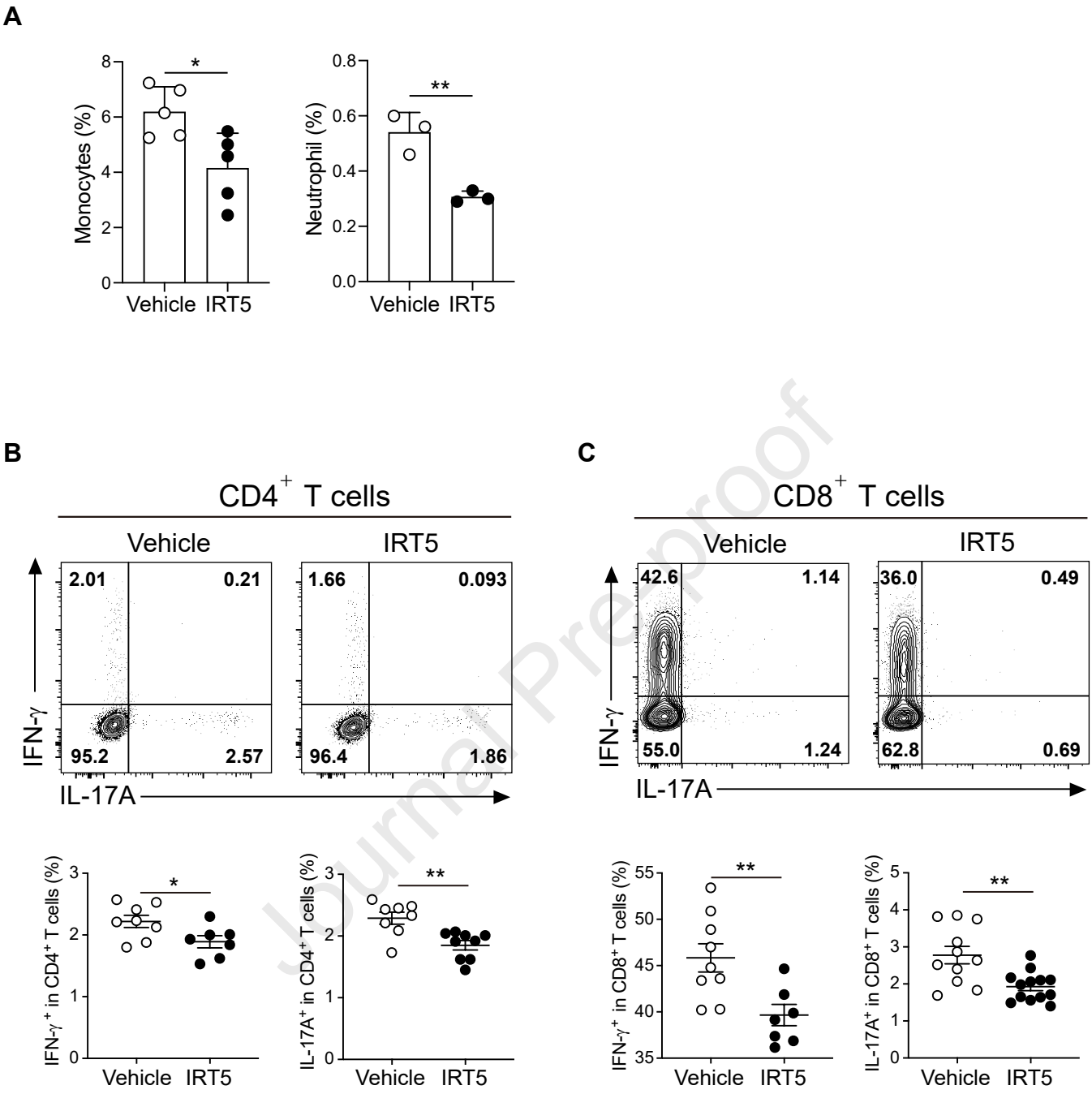

A

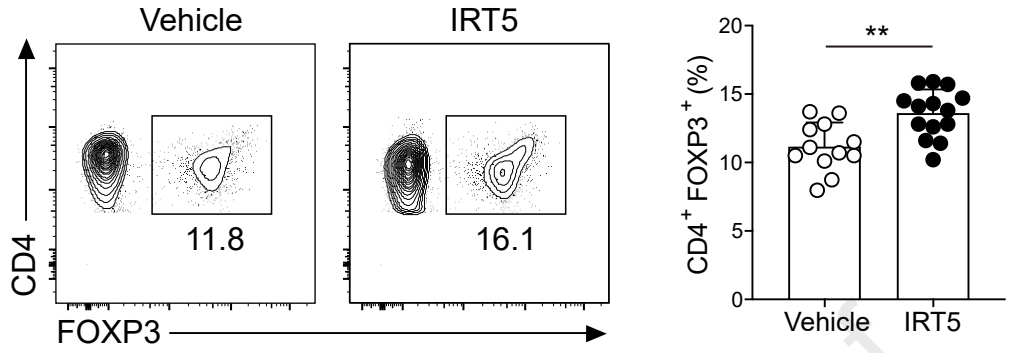

B

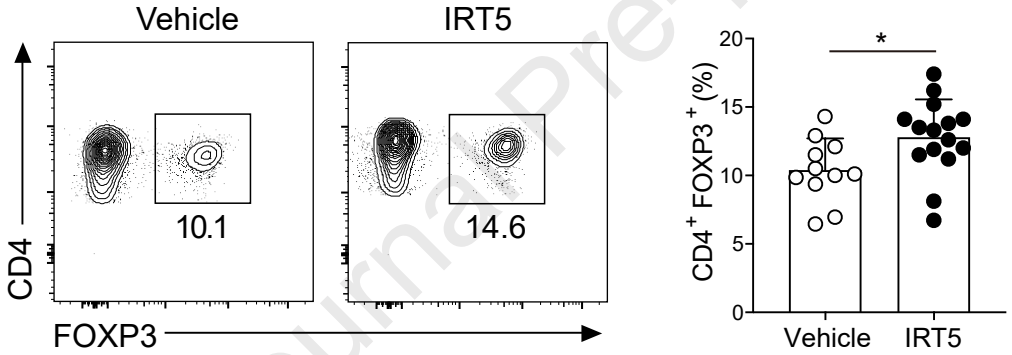

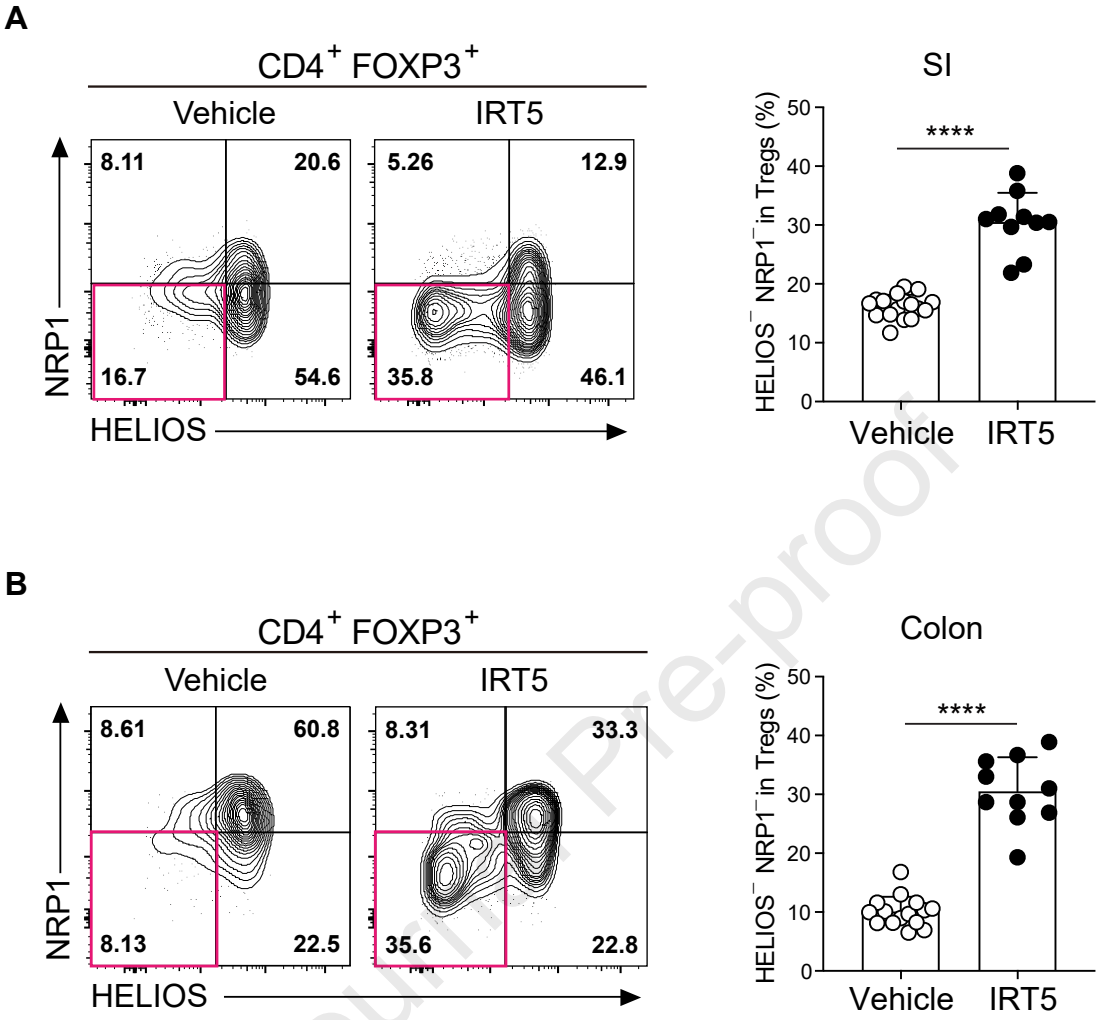

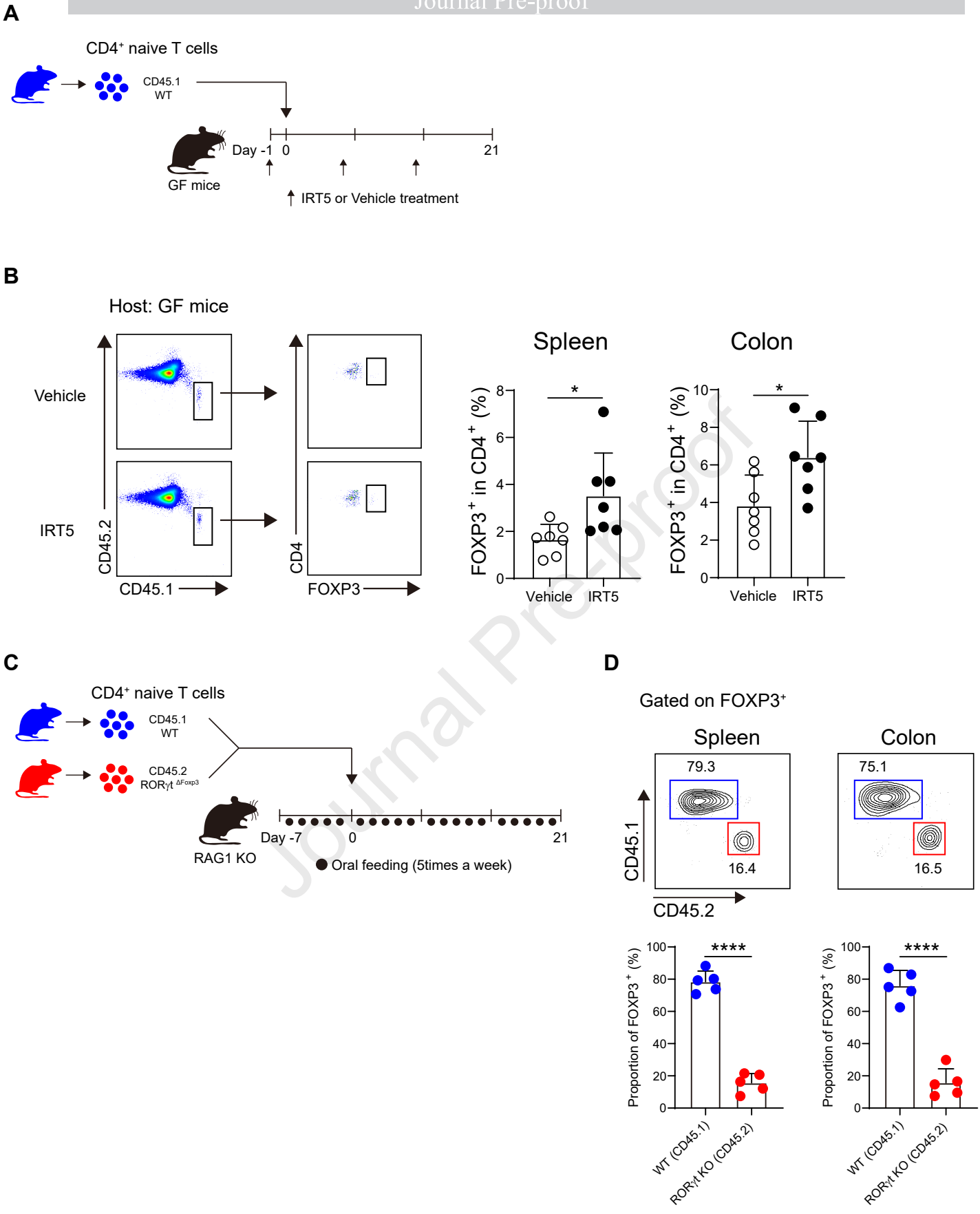

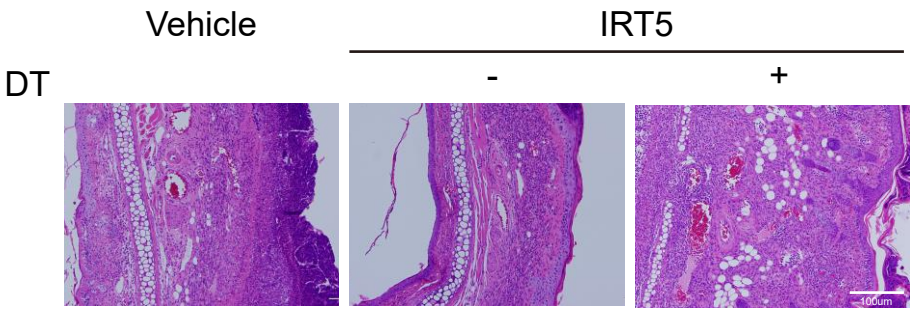

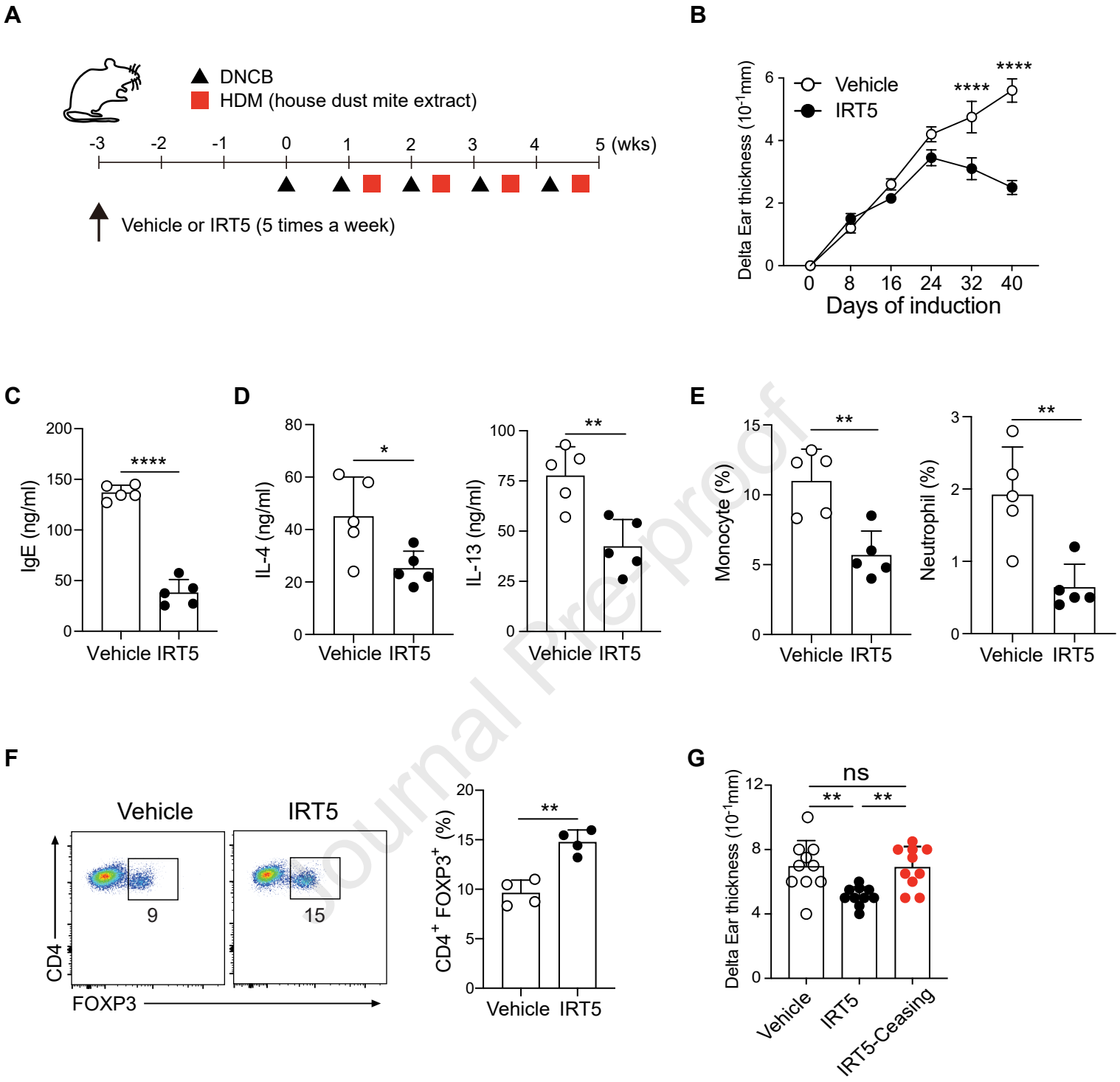

A

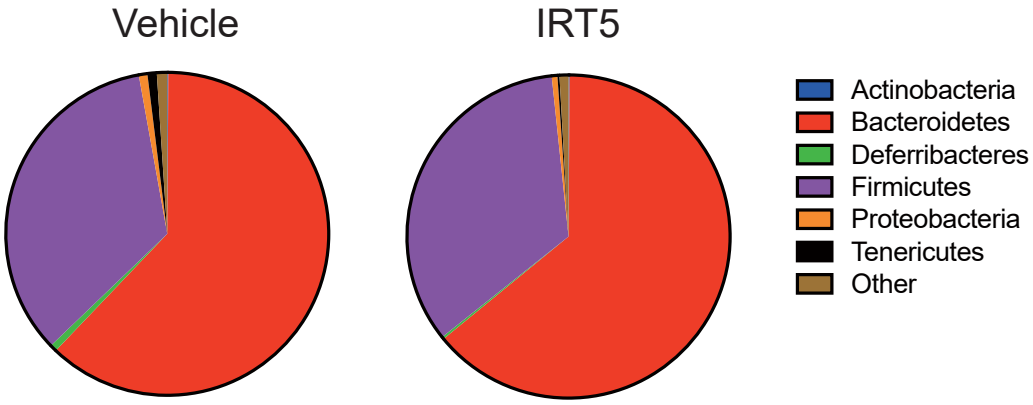

B

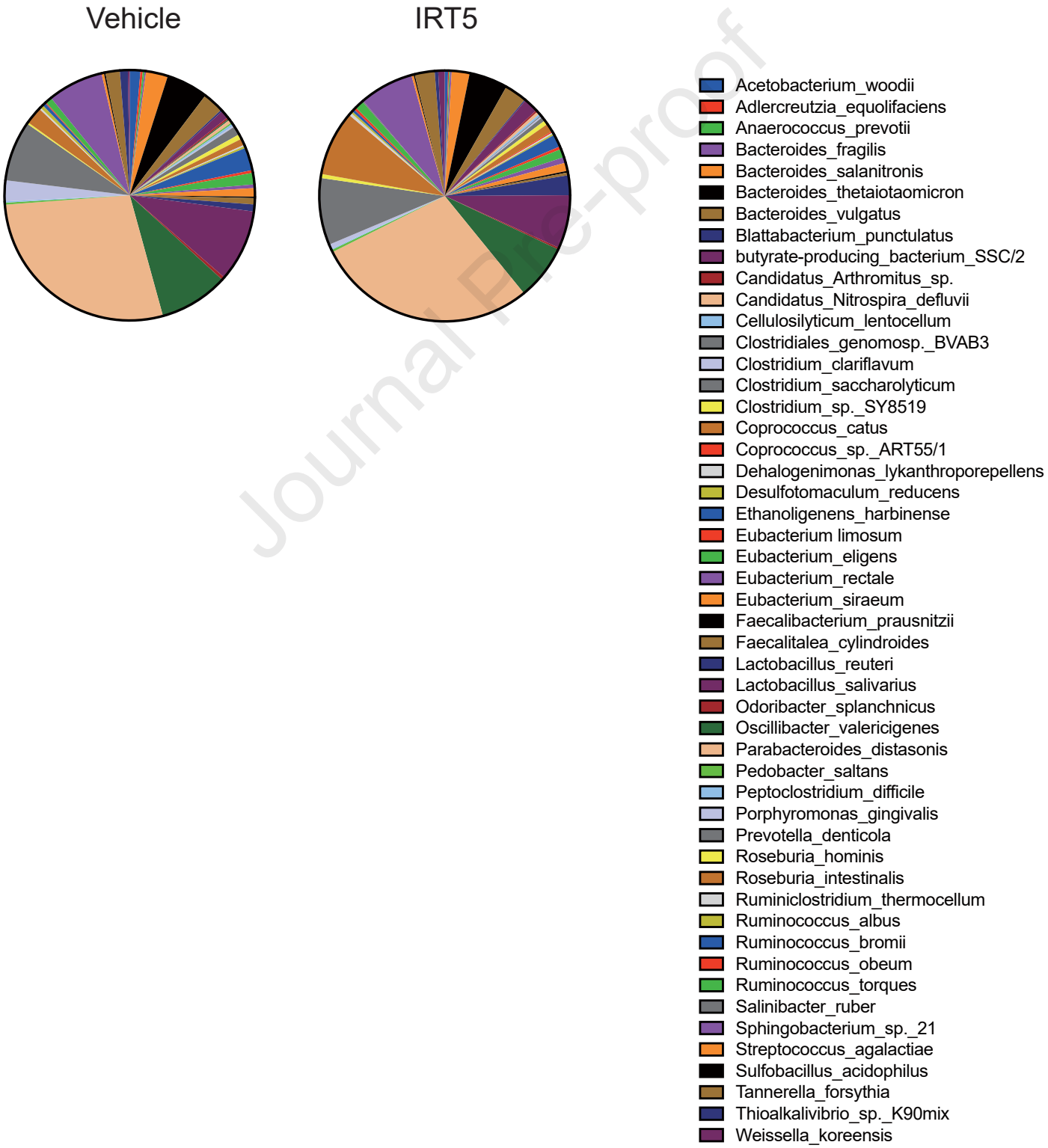

A

Cecal contents (μmole /g)	PBS	LA	LC	LR	ST	BB	IRT5
Butyrate	0	0	0	0	0	0	0

B

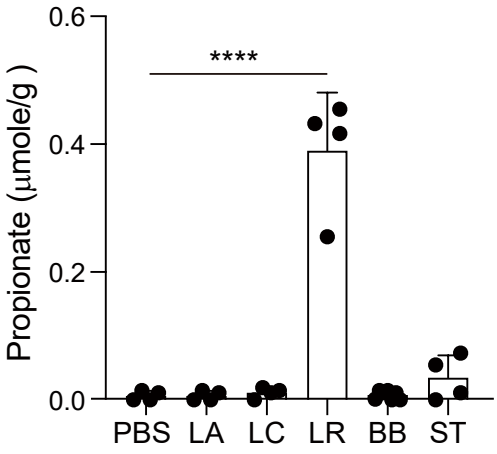

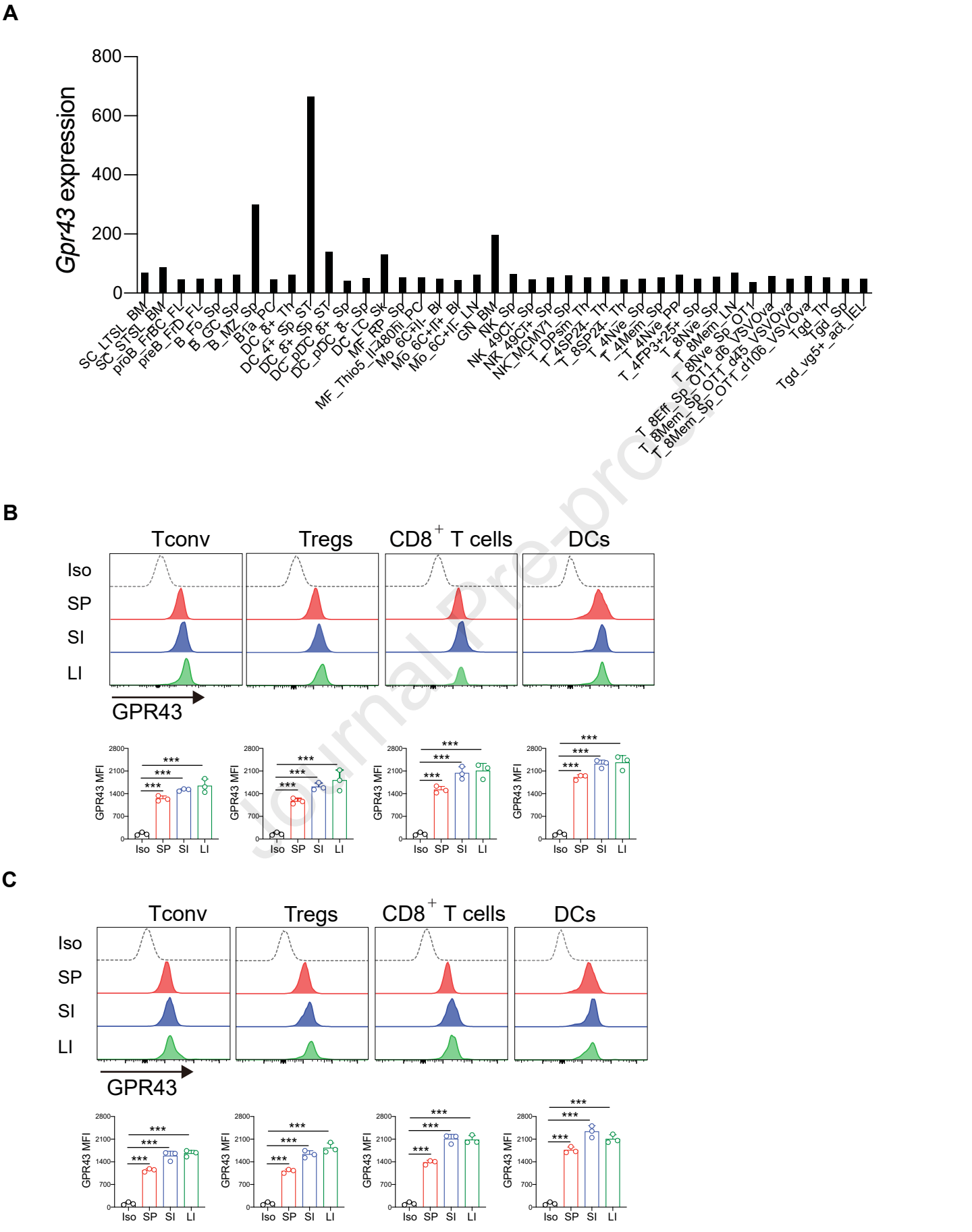

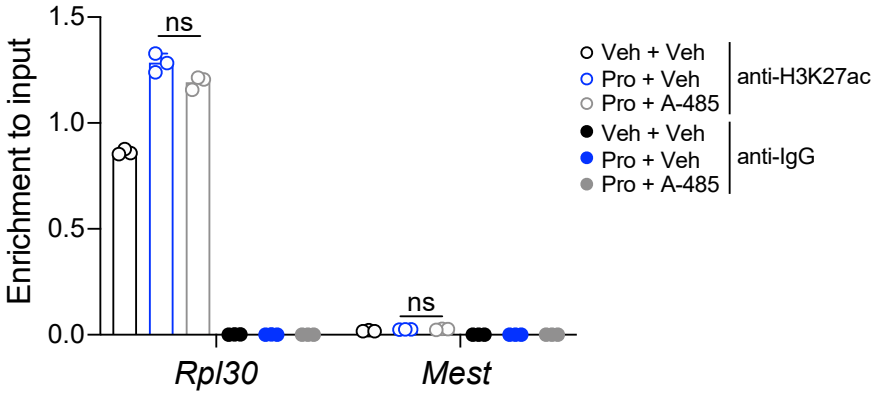

A

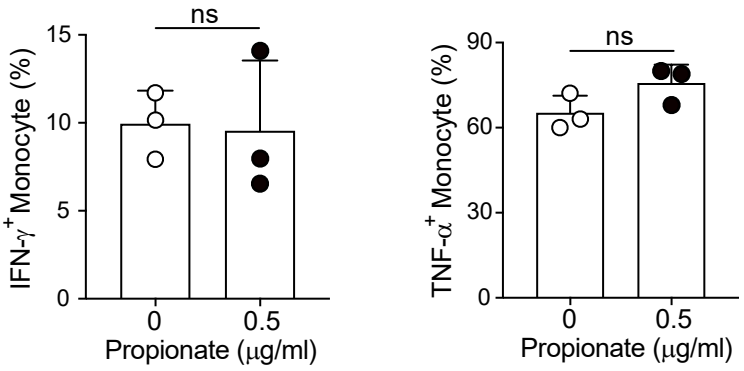

B

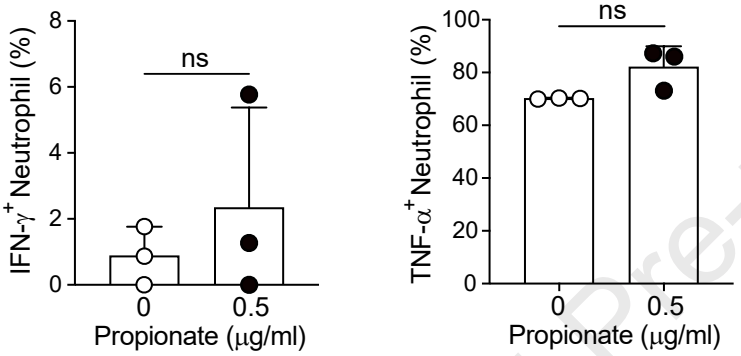

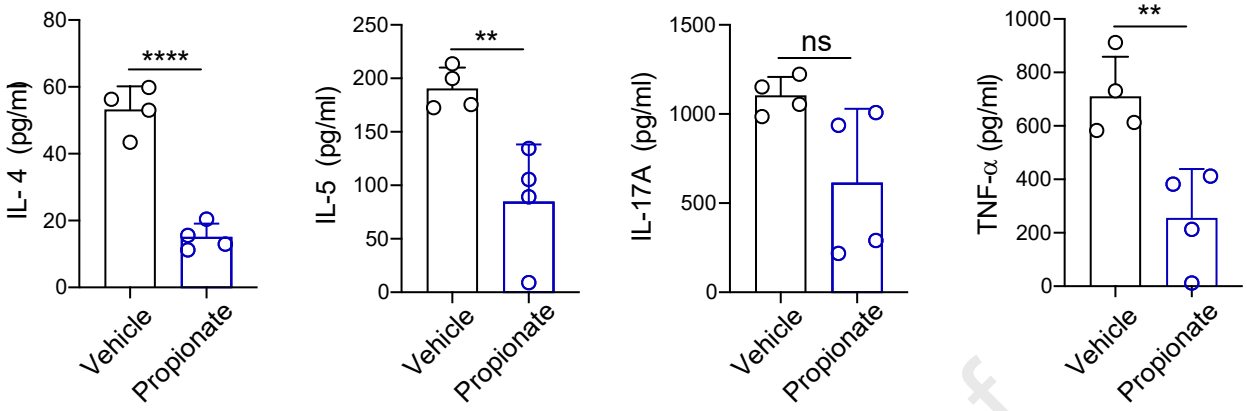

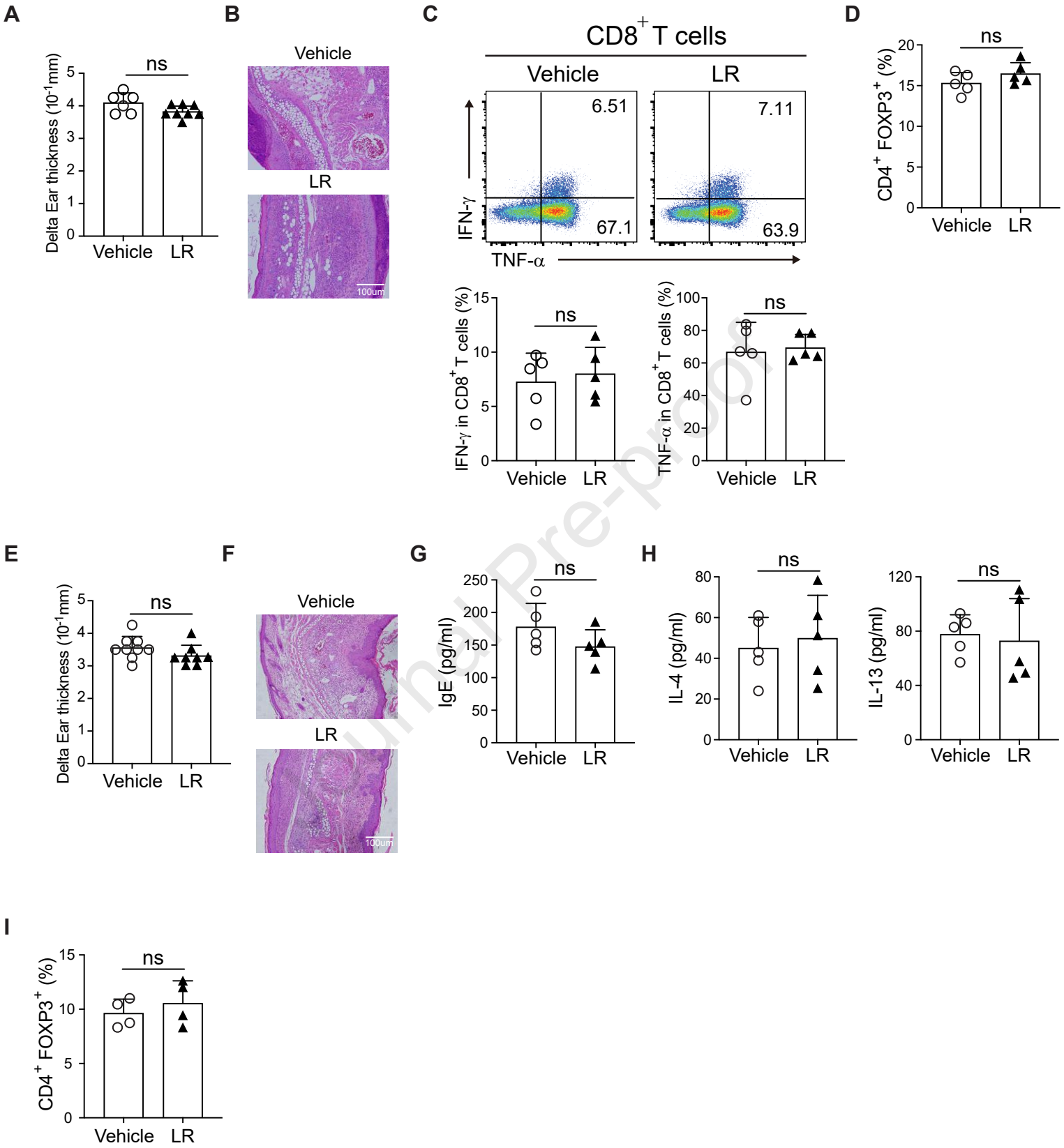

A

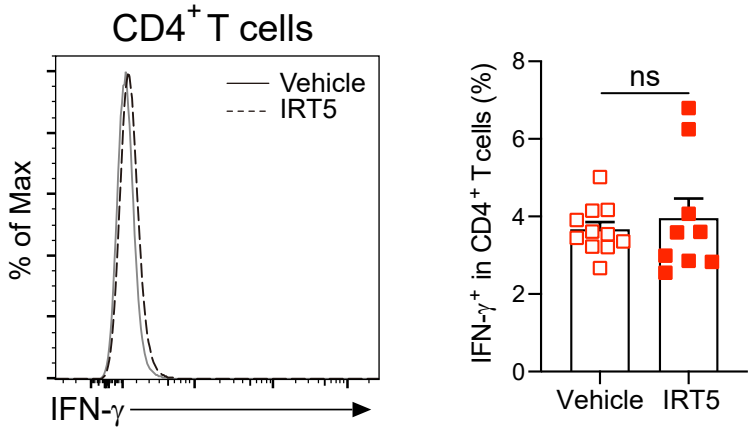

B

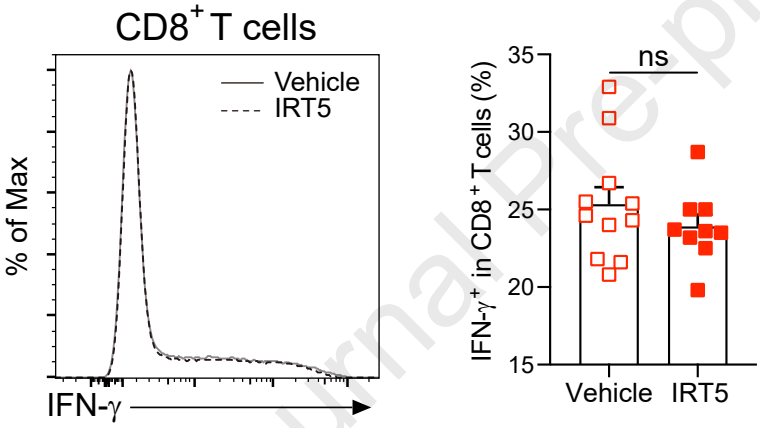

Materials and Methods

Mice

BALB/c mice were purchased from Hyochang Bio-Science (Daegu, Korea). C57BL/6, *Foxp3*^{DTR}, *Foxp3*^{cre}, *Rorc*^{flox}/*Foxp3*^{cre}, and *Rag*1$^{-/-}$ were originally obtained from Jackson laboratory. *Gpr*43$^{-/-}$ mice were kindly provided by Dr. Ikuno Kimura (Tokyo University, Japan). All animals were maintained in pathogen-free conditions in the animal facility. Germ free (GF) C57BL/6 (B6) mice obtained from Dr. Andrew Macpherson (Bern Univ., Switzerland) and Dr. David Artis (Cornell University, USA) was established and maintained in sterile flexible film isolators (Class Biological Clean Ltd., USA). All experimental procedures were performed in accordance with protocols approved by Animal Care and Ethics Committees of POSTECH Institutional Animal Care and Use Committee.

Probiotic strains

The IRT5 probiotics contains 1 x 10^8 cfu/g of each strain consisting of *Lactobacillus casei*, *Lactobacillus acidophilus*, *Lactobacillus reuteri*, *Bifidobacterium bifidum,* and *Streptococcus thermophiles* (final 5 x 10^8 cfu/ treatment).

Murine skin allergy models

For contact hypersensitivity (CHS), mice were sensitized by topical application of 100 μl of 4% of 2,4-Dinitrochlorobenzene (DNCB) (Sigma Aldrich) dissolved in acetone/olive oil solution (acetone: olive oil = 3: 1) at Day 0. After 7 days of sensitization, mice were repeatedly challenged with 20 μl of 1% DNCB or PBS in both ears twice a week at 3 days interval until 4 weeks. After 12 hrs of every challenging, ear thickness and clinical symptoms were monitored. Atopic dermatitis

(AD) was induced with house dust mite extract followed by previous study with minor modification[3]. Briefly, each ear was painted 2 times per weeks with DNCB or HDM extract repeatedly for 4 weeks. First, 20 μl of 2% DNCB, dissolved in acetone/olive oil (1:3) solution, was painted on each ear. After 4 days of DNCB painting, 20μl of 10 mg/ml HDM extract (GREER LABORATORIES INC) in 0.5% Tween-20/PBS solution was repainted, after 4 days. These treatments were repeated for 4 weeks. For Tregs depletion, after two times of DNCB challenge, IRT5 treated FoxP3^{DTR} mice were divided into two groups and injected with 20ng/g of diphtheria toxin (Sigma) or same volume of vehicle 3 times in every three days before sacrificing mice.

Histology

Ear tissues were collected and fixed in 4% formaldehyde for 12 hrs, embedded in paraffin blocks, sectioned at 3μm thickness, and stained with hematoxylin (Sigma Aldrich) and eosin (Sigma Aldrich).

Cell isolation

For the isolation of primary immune cells, splenic or local draining lymph nodes (dLNs; superficial and cervical lymph nodes) were used according to each experimental purpose. To isolate $CD4^+$ T cells or $CD11c^+$ DCs, isolated splenic or lymph node total cells were incubated with cell type specific isolation beads: Mouse $CD4^+$ T cell negative selection kit (Stem cell Technology, USA), mouse CD11c microbeads ultrapure (Miltenyi Biotech, Germany), or Sony cell sorter (SONY) by following manufacture's protocols. To isolate cells from inflamed tissues, ear tissues were cut into four pieces and gently stirred in flasks with solution (PBS containing 25 ml 10 mM EDTA, 3% FBS (HyClone Laboratories), 20mM HEPES and 1mM sodium

pyruvate) for 20 min at 37°C. The segments were washed three times with PBS and digested with 5 ml RPMI 1640 containing 1 mg/ml of type V collagenase (Sigma Aldrich) for 45 min at 37°C. Finally, the soup containing ear total cell was centrifuged and cultured in T cell media.

Adoptive transfer of naïve T cells

For germ-free (GF) transfer experiments, naïve $CD4^+$ T cells (1×10^6) from CD45.1 mice were intravenously injected into CD45.2 recipient mice in GF. After cell transfer, recipient mice were divided into two groups and treated with vehicle or IRT5 for 3 weeks, respectively. In $Rag1^{-/-}$ transfer experiments, naïve $CD4^+$ T cells ($CD4^+CD25^-CD44^{lo}CD62L^{hi}$) were prepared from spleens of CD45.1 WT or *Rorc*^{flox}/*Foxp3*^{cre} ($Rorc^{\Delta Foxp3}$) mice. Naïve $CD4^+$ T cells (5×10^5 cells from WT and $Rorc^{\Delta Foxp3}$) were co-transferred into *Rag1*$^{-/-}$ mice, gavaged with IRT5 for 3 weeks after cell transfer.

RNA Isolation, cDNA synthesis, quantitative RT-PCR

Total RNA was isolated from each samples and reverse transcription was performed with reverse transcriptase (Promega, USA) primed with oligo (dT) primer as previously described[3]. The synthesized cDNAs were amplified by real-time PCR and standard PCR with primer sets; IL-1β (F: GCAACTGTTCCTGAACTC AACT, R: ATCTTTTGGGGTCCGTCAACT), IL-6 (F: GAGGATACCACTCCCAACAGA CC, R: AAG TGCATCATCATCGTTGTTCA), IL-10 (F: ATAACTGCACCCACTTCCCA, R: TCATTTCCGATAAGGCTTGG), IL-12 (F: GGAAGCACGGCAGCAGAATA, R: AACTTGAGGGAGAAGTAGGAATGG), IL17A (F: TTCATCTGTGTCTCTGATGCT, R: TTGACCTTCACATTCTGGAG), IL-23 (F: TGGCATCGAGAAACTGTGAGA, R: TCAGTTATTGGTAGTCCTGTTA), IFN-ɣ (F: TCAAGTGGCATAGATGTGGAAGAA,

R: TGGCTCTGCAGGATTTTCATG), TNF-α (F: CATCTTCTCAAAATTCGAGTGACAA, R: TGGGAGTAGACAAGGTACAACCC), TGF-β (F: GAAGGCAGAGTTCAGGGT CTT, R: GGTTCCTGTCTTTGTGGTGAA), HPRT (F: TTATGGACAGGACTGAAA GAC, R: GCTTTAATGTAATCCAGCAGGT),

Cytokine measurement by ELISA

To determine cytokine production, ear total cells and dLN cells were stimulated with PMA and ionomycin for 4 hours and supernatants were collected. 100 µl of collected supernatant or diluted serum (1/200 ratio) was used for the detection of IL-1β, IL-2, IL-6, IL-10 levels (Koma Biotech), IL-12p40, IL-17a, IFN-γ and TGF-β (eBioscience) according to manufacturer's protocols.

Flow cytometric analysis

For the surface marker staining, cells were washed with ice-cold PBS, re-suspended in 100 µl of PBS and stained with anti-CD4-BUV395, anti-CD45.1-Percp5.5 (eBioscience), anti-CD8α-PE/Cy7 (TONBO), anti-CD11c-APC, anti-CD103-BV421, anti-CD11B-FITC, anti-LY6C-APC/Cy7, anti-LY6G-BUV510, anti-CD45.2-APC, anti-TCRβ-BV605, anti-CD4-APC/Cy7 (Biolegend), anti-NRP1-APC (R&D system), and anti-GPR43-Alex647 (Bioss). Cells were fixed and permeabilized with 1X Fixation/Permeabilization Concentrate and stained anti-TBET-APC, anti-RORγT-PE, anti-FOXP3-PE, anti-FOXP3-FITC (eBioscience), anti-HELIOS-Alexa Flour 488 and anti-CTLA4-BV421 (Biolegend). For intracellular cytokine stain, cells were permeabilized with IC fixation buffer (eBioscience) and stained with anti-IFN-γ-Alexa488 (eBioscience), anti-IL-17A-APC, or anti-IL-10-BV421 (Biolegend). The stained cells were analyzed on LSRFortessa or FACSCelesta (BD) flow cytometer

and the data were further analyzed with FlowJo software. To minimize the loss of cells during LP preps, LP cells were stained with Larminar Wash Mini1000 (Curiox).

iTregs generation

In vitro iTregs were generated by generation was performed with $CD4^{+}CD44^{lo}CD62L^{hi}CD25^{-}$ naïve T cells in presence or absence of $CD11c^{+}$ dendritic cells. 1) Presence of DCs: DCs was incubated with or without propionate (0.5μg/ml) for 14h in presence of 10 ng/ml of GM-CSF. Naïve T cells were incubated with these pretreated DCs with 10 ng/ml of GM-CSF, 0.1 ng/ml of TGF-β, 100 U/ml of IL-2 and 0.1 μg/ml of anti-CD3 for 3 days. 2) Absence of DCs: Naïve $CD4^{+}$ T cells was stimulated with immobilized anti-CD3 and anti-CD28 supplemented with 1 ng/ml of TGF-β together with vehicle or propionate (0.5μg/ml) with or without A-485 (0.3μM) for 4 days.

ChIP-qPCR analysis

ChIP-qPCR was performed as previously described[E3]. In brief, cells were treated with vehicle or propionate in the absence or presence of HAT inhibitor, washed with PBS and were cross linked with formaldehyde at final concentration 1% and fragmented chromatin were incubated with the acetylated H3K27 antibody (Abcam, ab4729) or rabbit IgG (Vector Laboratories, I-1000) for immunoprecipitation at 4 °C overnight. Ab/DNA complexes were reverse cross-linked by heat and the DNA was eluted by spin column. Real time PCR was performed to verify presence of selected DNA sequences using following primers: Foxp3 promoter (F: CACTCAGAGACTCGCAGCAG; R: GGGGTAGTGCTCTGTCTCCA), CNS1 (F: TGTTGGCTTCCAGTCTCCTT; R: TGCTGAGCACCTACCATCAT), Rpl30 (Cell

Signaling Technology, #7015), Mest (Cell Signaling Technology, # 12928). DNA purified from chromatin before immunoprecipitation was used as input. Data are presented as the amount of DNA recovered relative to the input control. Results with IgG was confirmed as background value showing <0.01 of relative ratio to input.

SCFA analysis

Sample was weighed (~ 100 mg dry matter) and a solution, composed by oxalic acid (0.1 mol/L), sodium azide (40 μmol/L), was added as 3 times volume (~ 300 μl). These were incubated at RT with shaking for 1h and then centrifuged (10 min at 16,000g). Supernatant was used for analyze of SCFA concentration using an HPINNOWax column (30 m × 0.25 mm, 0.25 μm film thickness). Concentration of SCFA was determined with gas chromatography (Shimadzu GC2010, Japan) and quantified by comparing their peak areas with the standards. The change in relative SCFA levels was calculated by concentration of each SCFA divided by the sum of total concentration of SCFAs in each sample.

DNA extraction, 16S rRNA amplification and Miseq sequencing

Fresh stools were collected before mice were sacrificed. DNA was extracted using PowerSoil® DNA Isolation Kit (QIAGEN) according to manufacturer's protocol. Each sample was prepared according to the Illumina 16S Metagenomic Sequencing Library protocols (version of Illumina). The quantity and quality of DNA were measured by PicoGreen and Nanodrop. The 16S rRNA genes were amplified using following primers: 16S V3-V4 (F: TCGTCGGCAGCGTCAGATGTGTATAAGAGACAGCCTACGGGNGGCWGCAG; R: GTCTCGTGGGCTCGGAGATGTGTATAAGAGACAGGACTACHVGGGTATCTAA

TCC). A sub-sequent limited-cycle amplification step is performed to add multiplexing indices and Illumina sequencing adapters. The final products are normalized and pooled using the PicoGreen, and the size of libraries are verified using the TapeStation DNA screentape D1000 (Agilent). Those were sequenced using the MiSeq™ platform (Illumina, San Diego, USA). Potentially chimeric sequences were removed using CD-HIT-OUT. The non-chimeric sequences were analyzed in the QIIME (v1.8) using operational taxonomic units (OTUs) grouped by operational taxonomic units (OTUs).

Statistical Analysis

For statistical analyses, all experiments were performed more than three times. Statistical analyses were performed using Prism (GraphPad Software) by the unpaired Student's t test or two-way ANOVA with two-way ANOVA with Bonferroni's multiple comparisons. The significant differences were indicated with p-Values below 0.05 in the following manner: *, $p \leq 0.05$; **, $p \leq 0.005$; ***, $p \leq 0.0005$; ****, $p \leq 0.0001$. All inclusion of statistical analyses is indicated in the figure legends of main and supplementary figures.

176

177 **Figure legends**

178 **Figure E1. Prophylactic effect of probiotics in CHS induced mice.** Upon vehicle
179 or IRT5 treatment, (A) the change of infiltrated monocyte and neutrophil at inflamed
180 site and the level of IFN-γ and IL-17A production (B) $CD4^+$ and (C) $CD8^+$ T cells from
181 dLNs in CHS induced mice. Representative FACS plots of each group. Each dot
182 represents individual animal from 3 independent experiments. Graphs show mean
183 +/- s.e.m. *p < 0.05, ***p < 0.01, ***p < 0.005 calculated by student t-test.

184

185 **Figure E2. Probiotics induce $CD4^+Foxp3^+$ Tregs in CHS-induced mice.** Tregs
186 frequency in (A) dLNs and (B) small intestine of vehicle or IRT5 treated CHS mice.
187 Representative FACS plots of each group. Each dot represents individual animal
188 from 3 independent experiments. Error bars denote means ± s.e.m. Graphs show
189 mean +/- s.e.m. *p < 0.05, ***p < 0.01, ***p < 0.005 calculated by student t-test.

190

191 **Figure E3. Probiotics specifically induce $HELIOS^-NRP1^-$ Tregs.** HELIOS and
192 NRP1 expression in (A) small intestinal and (B) colonic Tregs from vehicle or IRT5
193 treated germ-free mice. Representative FACS plots of each group. Each dot
194 represents individual animal from 3 independent experiments. Error bars denote
195 means ± s.e.m. Graphs show mean +/- s.e.m. *p < 0.05, ***p < 0.01, ***p < 0.005
196 calculated by student t-test.

197

198 **Figure E4. IRT5 administration induces the conversion of naïve $CD4^+$ T cells**
199 **into Tregs.** (A) Experimental scheme of naïve T cells transferring experiment. (B)
200 Proportion of converted Tregs from the transferred naïve T cells in spleen or colon

upon vehicle or IRT5 treatment. (C) Experimental scheme of co-transferring experiments of WT or *Rorc*^{flox}/*Foxp3*^{cre} naïve T cells. (D) The proportion of converted Tregs from WT or *Rorc*^{flox}/*Foxp3*^{cre} naïve T cells in spleen and colon after 3 weeks treatment of IRT5. Representative FACS plots of each group. Each dot represents individual animal from 3 independent experiments. Error bars denote means ± s.e.m. Graphs show mean +/- s.e.m. *p < 0.05, ***p < 0.01, ***p < 0.005 calculated by student t-test.

Figure E5. Abrogation of therapeutic potency of IRT5 by Tregs depletion. CHS induced WT and *Foxp3*^{DTR} mice were treated with vehicle or IRT5 for 5 weeks. After weeks of treatment, *Foxp3*^{DTR} mice were divided into two groups and injected with vehicle or diphtheria toxin to deplete Tregs. All groups were sacrificed and the histological status of the inflamed tissue was confirmed by H&E staining in each group. Representative histology picture of each group from 5~10 animals in 3 independent experiments.

Figure E6. IRT5 suppresses atopic dermatitis. (A) Experimental scheme: mice were pre-treated with vehicle or IRT5 for three weeks, and induced AD by the repeated painting of DNCB and HDM for five weeks together with vehicle or IRT5 treatment. After 5 weeks of AD duction, (B) ear thickness, (C) serum IgE, (D) serum T_H2 cytokines (IL-4 and IL-13), (E) monocyte or neutrophil infiltration, and (F) Tregs proportion at inflamed tissue were analyzed in vehicle or IRT5 treated mice. (G) Ear thickness of AD mice treated with vehicle or IRT5 just before or a month before AD induction. Each symbol represents individual animal and performed at least 3

independent experiments. Graphs show mean +/- s.e.m. *p < 0.05, ***p < 0.01, ***p < 0.005 calculated by student t-test.

Figure E7. No overall change in microbiome composition by IRT5 treatment in CHS mice. After treatment of vehicle or IRT5 in CHS mice, stools were collected from each group, gut microbiome composition (relative OTU composition) were analyzed by 16S ribosomal RNA sequence, and sorted at (A) the phylum and (B) species level.

Figure E8. SCFAs production after colonization of individual probiotic bacteria in germ-free mice. After colonization of mock or each bacterial strain, fecal (A) butyrate and (B) propionate concentration was measured. Data represents average concentration of each SCFA from 5~10 animals in 3 independent experiments. Graphs show mean +/- s.e.m. *p < 0.05, ***p < 0.01, ***p < 0.005 calculated by one-way ANOVA with Tukey post hoc tests.

Figure E9. Grp43 expression in immune cells. (A) *Gpr43* expression of various DCs and T cells in Immgen database (http://www.immgen.org/). GPR43 expression on Tconv, Tregs, $CD8^+$ T cells, and DCs in spleen, SI, and colon were analyzed in (B) CHS or (C) AD induced mice. Each symbol represents individual animal and performed at least 3 independent experiments. Graphs show mean +/- s.e.m. *p < 0.05, ***p < 0.01, ***p < 0.005 calculated by student t-test.

Figure E10. H3K27 acetylation at Rpl30 and Mest using ChIP-qPCR. Data is average of 3 independent experiments. Error bars denote means ± s.e.m. Graphs show mean +/- s.e.m. *p < 0.05, ***p < 0.01, ***p < 0.005 calculated by student t-test.

Figure E11. Propionate effects on monocyte and neutrophil. Production of IFN-γ/TNF-α by (A) monocyte or (B) neutrophil sorted from CHS induced mice upon treatment of vehicle or propionate. Each symbol represents individual animal and performed at least 3 independent experiments. Graphs show mean +/- s.e.m. *p < 0.05, ***p < 0.01, ***p < 0.005 calculated by student t-test.

Figure E12. Propionate suppresses pathogenic cytokines in AD. Production of IL-4, IL-5, IL-17A, and TNF-α by $CD4^+$ T cells from AD induced mice upon treatment of vehicle or propionate. Data is average of 3 independent experiments. Error bars denote means ± s.e.m. Graphs show mean +/- s.e.m. *p < 0.05, ***p < 0.01, ***p < 0.005 calculated by student t-test.

Figure E13. LR alone is not sufficient to recapitulate therapeutic potency of IRT5 in CHS and AD. After treatment of vehicle or LR in CHS induced mice, (A) ear thickness, (B) histological feature, (C) IFN-γ/TNF-α production in $CD8^+$ T cells, and (D) Tregs proportion at inflamed tissue were analyzed. After treatment of vehicle or LR in AD induced mice, (E) ear thickness, (F) histological feature, (G) IgE, (H) IL-4/IL-5 level in serum, and (I) Tregs proportion at inflamed tissue were analyzed. Each symbol represents individual animal and performed at least 3 independent experiments. Graphs show mean +/- s.e.m. *p < 0.05, ***p < 0.01, ***p < 0.005 calculated by student t-test.

Figure E14. Impaired suppression of CHS progression by IRT5 in *Gpr*43 KO mice. Production of IFN-γ by (A) $CD4^+$ T cells or (B) $CD8^+$ T cells from dLNs of CHS-induced Gpr43 KO mice treated with vehicle or IRT5. Representative FACS plots of each group. Each dot represents individual animal from 3 independent experiments. Error bars denote means ± s.e.m. *p < 0.05, ***p < 0.01, ***p < 0.005 calculated by student t-test.